DALTON
FULL PAPER

First mixed valence cerium–organic trinuclear cluster $[Ce_3(OBu^t)_{10}NO_3]$ as a possible molecular switch: synthesis, structure and density functional calculations

Yurii K. Gun'ko,*[a] Simon D. Elliott,†[a] Peter B. Hitchcock[b] and Michael F. Lappert*[b]

[a] *The Department of Chemistry, Trinity College Dublin, Dublin 2, Ireland. E-mail: igounko@tcd.ie*
[b] *The Chemistry Laboratory, University of Sussex, Brighton, UK BN1 9QJ. E-mail: M.F.Lappert@sussex.ac.uk*

Received 9th November 2001, Accepted 4th February 2002
First published as an Advance Article on the web 20th March 2002

The crystalline trinuclear cerium cluster complex $[\{(Ce(OBu^t)_2\}_2(\mu\text{-}OBu^t)_3(\mu_3\text{-}OBu^t)_2\{Ce(OBu^t)(NO_3)\}]$ **1** has been obtained in good yield from $2[Ce(OBu^t)_4(thf)_2]$, $[Ce(OBu^t)_3(NO_3)]$ and $Sn(C_5H_3Bu^t_2\text{-}1,3)Me_3$ by refluxing in hexane, and was characterised by microanalysis, ^{1}H NMR, IR and UV–Vis spectra and MS data. Its structure and bonding have been analysed by X-ray diffraction. Density functional calculations were carried out on the model compound **2**, in which each OBu^t substituent was replaced by OH, and **3**, related to **2** but with OH instead of NO_3. The geometric parameters showed good agreement with experiment. It is concluded that **1** is a mixed valence Ce(III)[Ce(IV)]$_2$ cluster, that the single f electron is localised on the NO_3-bearing Ce atom, and that excitation of this electron to a low energy alternative state is facile. Hence the cluster may offer potential as an f-electron molecular switch.

Introduction

Molecular electronics is a fast developing area. Much research has focused on a variety of organic molecules,[1] but data on organometallic devices are scant. Mixed valence metallorganic clusters may be promising components for molecular electronics, because of their unique electronic properties.[2] We now report the synthesis and structural characterisation of the first mixed valence cerium–organic trinuclear cluster, and density functional calculations to support the discussion of its atomic and electronic structure.

Results

Synthesis and characterisation of $[\{(Ce(OBu^t)_2\}_2(\mu\text{-}OBu^t)_3(\mu_3\text{-}OBu^t)_2\{Ce(OBu^t)(NO_3)\}]$ 1

Treatment of two equivalents of $[Ce(OBu^t)_4(thf)_2]$ and one equivalent of $Ce(OBu^t)_3(NO_3)$[3] with an excess of $Sn(C_5H_3Bu^t_2\text{-}1,3)Me_3$ under reflux in hexane reproducibly afforded the green–brown, crystalline trinuclear cluster complex **1** in good yield, eqn. (1):

$$2[Ce(OBu^t)_4(thf)_2] + Ce(OBu^t)_3(NO_3) + 3Sn(C_5H_3Bu^t_2\text{-}1,3)Me_3 \longrightarrow [\{Ce(OBu^t)_2\}_2(\mu\text{-}OBu^t)_3(\mu_3\text{-}OBu^t)_2\{Ce(OBu^t)(NO_3)\}] \quad (1)$$

Complex **1** was characterised by satisfactory microanalytical data, as well as ^{1}H NMR, EI-MS, UV–Vis and IR spectra, MS and single crystal X-ray diffraction data (*vide infra*). The ^{1}H NMR spectrum in benzene-d_6 showed three weakly [$\delta\{^1H\}$ 3.15, 1.44, 1.24] and four strongly [$\delta\{^1H\}$ 17.34, 8.55, −4.68, −7.40] paramagnetically shifted signals of the Bu^t protons.The UV–Vis spectrum in toluene had strong absorptions at λ = 220, 258, 278 and 336 nm.The IR spectrum displayed absorption maxima at ν = 1513, 1028, 771 and 744 cm^{-1}, assigned to the $[NO_3]^-$ ligand. The EI-MS spectrum had a strong peak at m/z = 1093, assigned to $[\{Ce(OBu^t)_3\}_3O]^+$.

Crystal structure of 1

Single crystals of **1** were obtained as the *n*-hexane solvate by crystallisation from hexane. The molecular structure is illustrated in Fig. 1 and selected bond lengths and bond angle are presented in Table 1. The structure has a central core of three cerium atoms, arranged in an almost equilateral triangle, which are joined to one another by three doubly bridging and two triply bridging $[OBu^t]^-$ ligands. The cerium atom Ce1 has a single, while each of Ce2 and Ce3 has two terminal $[OBu^t]^-$ ligands. The coordination environment about Ce1 is completed by an *O*,*O*′-chelating $[NO_3]^-$ ligand. The Ce1–Ce(2 or 3)

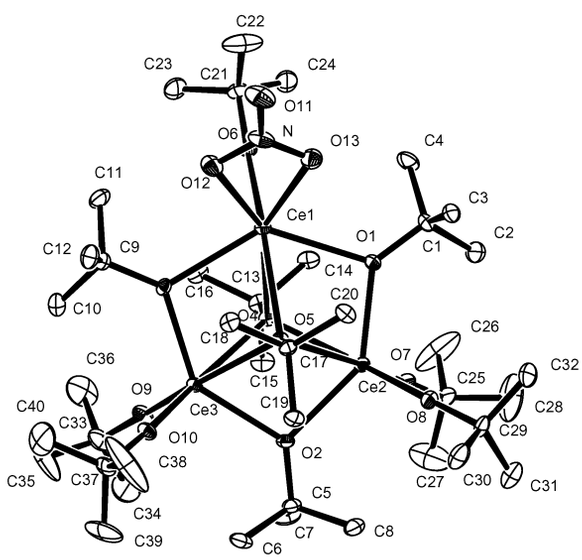

Fig. 1 X-Ray structure of **1**. H atoms have been omitted for clarity, the probability for the ellipsoids is ~20%.

† *Current address*: NMRC, University College Cork, Lee Maltings, Prospect Row, Cork, Ireland.

 DOI: 10.1039/b110247h

Table 1 Selected geometric parameters (bond length/Å or angle/°) for crystalline **1** (X-ray data) and for the model compounds **2** ("ground" $^2A'$ and "excited" $^2A''$ states) and **3** (UKS/SVP calculated data). Ce atom labels are as in Fig. 1; all of the listed O atoms are in hydroxy/butoxy ligands except where indicated as O(N)

	1	**2** $^2A'$	**2** $^2A''$	**3** $^2A'_1$
Ce1–Ce(2,3)	3.7277(6), 3.7249(7)	3.71	3.63	3.68
Ce2–Ce3	3.6828(7)	3.62	3.74	3.68
Ce1–N	2.996(5)	2.96	2.92	—
Ce1–O(N)	2.574(4), 2.564(5)	2.52	2.46	—
κ^1-Ce1–O	2.141(6)	2.12	2.05	2.09
κ^1-Ce(2,3)–O	2.062(4)–2.069(4)	2.07, 2.08	2.10, 2.10	2.09
μ-Ce1–O	2.501(4), 2.519(4)	2.51	2.26	2.33
μ-Ce(2,3)–O	2.261(4)–2.364(4)	2.23, 2.35	2.36, 2.43	2.33
μ_3-Ce1–O	2.540(4), 2.620(3)	2.54, 2.62	2.33, 2.40	2.45
μ_3-Ce(2,3)–O	2.471(4)–2.505(4)	2.41, 2.44	2.53, 2.54	2.45
Ce2–Ce1–Ce3	59.23	58.4	62.0	60

distances of 3.726(2) Å are slightly longer than the 3.683(1) Å of Ce2–Ce3 and are significantly shorter than the Ce–Ce separation of 3.887(4) Å in $[\{Ce(\eta^5\text{-}C_5H_3Bu^t_2\text{-}1,3)_2(OMe)\}_2]$,[4] but are similar to three of the four Ce–Ce distances in $[Ce_4O(OPr^i)_7(\mu\text{-}OPr^i)_4(\mu_3\text{-}OPr^i)_2(\mu_4\text{-}O)(HOPr^i)]$ **A**, 3.66 ± 0.07 Å.[5]

The four terminal OBu^t–Ce(2 or 3) bond distances of 2.062(4)–2.069(4) Å in **1** are significantly shorter than the corresponding OBu^t–Ce1 bond length, 2.141(4) Å, but are similar to the OBu^t–Ce(IV) bond lengths in $[Ce(OBu^t)_2(NO_3)_2(HOBu^t)_2]$ **B**, 2.025 ± 0.003 Å,[3] and the terminal OPr^i–Ce bond lengths in **A**, 2.078(7) and 2.113(7) Å.[5] The μ-OBu^t–Ce bond distances in **1** decrease in the sequence Ce1–O(1 or 3) [2.501(4) and 2.519(4) Å] > Ce(2 or 3)–O2 [2.357(4) and 2.364(4) Å] > Ce2–O1 and Ce3–O3 [2.265(4) and 2.261(4) Å]. The four μ_3-OBu^t–Ce distances Ce(2 or 3)–O(4 or 5) in **1**, ranging from 2.471(4) to 2.505(4) Å, are shorter then the Ce2–O(4 or 5) of 2.540(4) and 2.620(3) Å. In **A**, the μ-OPr^i–Ce bond distances range from 2.298(6) to 2.390(6) and 2.483(5) to 2.524(6) Å, respectively.[5]

The nitrate ligand in **1** is bound in a κ^2-fashion to Ce1 with Ce–ON, N–OCe and terminal N–O bond lengths of 2.574(4) and 2.564(4), 1.270(7) and 1.260(7), and 1.220(7) Å, respectively. These values are similar to the corresponding parameters in (a) the Ce(IV) nitrate **B** [2.515(6), 2.529(6), 2.583(5) and 2.593(5); 1.254(8), 1.258(4), 1.260(8) and 1.277(9); and 1.207(8) and 1.235(8) Å, respectively],[3] (b) the cationic Ce(IV) nitrate $[NH_4]_2[Ce(NO_3)_6]$ [av. 2.508(7), 1.28(1) and 1.23(1) Å, respectively],[6] and in $[Ce(IV)(NO_3)_4(OPPh_3)_2]$ [av. 2.478, 1.27 and 1.23 Å, respectively].[7]

Computational studies

Two model compounds are considered for computation: the C_s-symmetric $[Ce_3(OH)_{10}NO_3]$ **2**, in which the $[OH]^-$ replaces the $[OBu^t]^-$ ligands of complex **1**, and the D_{3h}-symmetric $[Ce_3(OH)_{11}]$ **3** (Fig. 2).

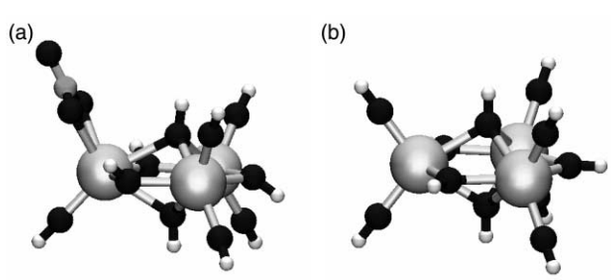

Fig. 2 Model compounds for calculations: (a) the C_s-symmetric **2** $[Ce_3(OH)_{10}NO_3]$ and (b) the D_{3h}-symmetric **3** $[Ce_3(OH)_{11}]$, showing Ce (large grey spheres), O (medium black), N (medium grey) and H (small white).

Calculations were carried out using Unretricted Kohn–Sham density functional theory (UKS) with a gradient-corrected functional, large basis set and a Ce effective core potential (*vide infra*). The geometries of **2** and **3** were optimised within symmetry constraints. Because each of the neutral complexes **1**–**3** is composed of three cerium ions and eleven uninegative ligands, it follows that each has a single Ce-centred f-electron and that they are doublets. One possible assignment of formal oxidation numbers in the cerium core is therefore +3, +4, +4. The f-character UKS molecular orbitals (MOs) of the symmetric Ce_3 core of **3** can form the σ-bonding combination $a'_1 + e'$. When the symmetry is lowered to C_s by the $[NO_3]^-$ ligand of **2**, these MOs split into $a' + a' + a''$. Thus, according to f-electron occupancy, **2** can assume either the $^2A'$ or $^2A''$ state, which we refer to as the "ground" and "excited" states respectively. As we are limited to single-determinant UKS, it is not possible to properly compute exited electronic states. We merely term the alternative $^2A''$ state as "excited" to distinguish it from the lower energy $^2A'$ state. Both states show completely filled MOs with no holes in occupancy.

Calculated geometries of **2** are compared with the X-ray diffraction data for **1** in Table 1. In **2**, two slightly different stable molecular geometries are found for the two doublet states ("ground" and "excited"): the difference in UKS energy is calculated to be just 18 kJ mol^{-1}. Despite the very slight differences between the two, it is indeed the geometry of the lower-energy $^2A'$ "ground" state, which matches experiment: all distances agree to within 0.07 Å (*i.e.* <2%) and the Ce–Ce–Ce angles to <1°. Perhaps the most important geometrical result is the very slight distortion to C_s (**2**) from D_{3h} (**3**) (<0.06 Å = 2% and <2° in Ce–Ce–Ce, <0.17 Å = 7% in Ce–O, Table 1).

Discussion

The reaction pathway to 1

The formation of the trinuclear cluster compound **1** by the procedure of eqn. (1) was unexpected. The original aim was to use the Ce(IV) precursor complexes as sources of Ce(IV) cyclopentadienyls. In the event, the tin(IV) reagent $Sn(C_5H_3Bu^t_2\text{-}1,3)Me_3$ evidently functioned as a reducing agent, either directly or, more probably, *via* an intermediate Ce(IV) cyclopentadienyl, which underwent facile homolysis generating a cyclopentadienyl radical and a transient Ce(III) *tert*-butoxide, which was trapped by two Ce(IV) monomeric species to yield **1**. As evidence we observed $SnMe_3(OBu^t)$ and $C_5H_4Bu^t_2$ among the coproducts.

Structure and bonding

The stoichiometry of **1**, along with the ^1H NMR, spectral data and the X-ray structural parameters, enables us to propose that the Ce1 atom is in the +3 oxidation state, while the other two Ce atoms are in the oxidation state +4. This is most readily demonstrated by examining the selected Ce–ligand distances in Table 1. For all of the butoxy ligands (terminal, bridging and

capping) the Ce–O distances are shorter to Ce2 and Ce3 than Ce1, consistent with the two former being the more highly charged cations. The same argument applies to the calculated structure of the $^2A'$ "ground" state of model compound **2**.

The picture is reversed in the $^2A''$ "excited" state of **2**. Here, Ce1 is more highly cationic (+4) and shows shorter distances to ligands. The charge on Ce(2) and Ce(3) is reduced by the f electron, so that they are further from the anions; lengthening of the bridging Ce–O causes Ce2–Ce3 to lengthen in this "excited" state.

The closest structure to **1** is the mixed valent tetranuclear cluster $[Ce_4O(OPr^i)_7(\mu\text{-}OPr^i)_4(\mu_3\text{-}OPr^i)_2(\mu_4\text{-}O)(HOPr^i)]$ **A**, in which, however, there was no clear distinction between the Ce(III) and Ce(IV) centres.[5]

Electronic structure

The effect of the $[NO_3]^-$ ligand is to lower the symmetry of the cluster from D_{3h} to C_s. This has important consequences for the electronic structure of the Ce_3 core, in particular for the lowest-lying MOs of Ce: f character. Whereas the homoleptic compound **3** shows delocalised two- and three-centre σ(f – f) MOs (Fig. 3), the lower symmetry of the heteroleptic **2** causes these MOs to localise on specific Ce atoms, Fig. 4.

As shown in Fig. 4, the "ground" $^2A'$ state of **2** has one f electron localised mainly on the $[NO_3]^-$ -bearing Ce1. This fits the classical picture: Ce(III)Ce(IV)Ce(IV) and supports the above discussion of the structure of **1**. In the "excited" $^2A''$ state of **2** the f electron is shared between Ce2 and Ce3, Fig. 5.

From exploratory calculations (not detailed here) on cationic and anionic versions of **3**, we find that additional f electrons cause both the Ce–Ce and Ce–O distances to increase slightly. This is consistent with the weaker ionic bonding expected from a less cationic metal core, and indicates that the f electrons do not play a major Ce–Ce or Ce–O covalent bonding role.

Evidence for the weakness of f–f interactions in the Ce_3 core comes from a number of sources. First and most important is the small UKS energy difference between the two states of **2** (ΔE = 18 kJ mol^{-1} = 0.18 eV, optimised geometries), indicating that occupancy of Ce f MOs has little direct effect on cluster stability. Second, the ostensibly σ-bonding MOs a'_1 + e′ of **3** are split by just 0.16 eV. This splitting may be the primary source of the ΔE between the "ground" and "excited" states of **2**. More evidence for weak f–f interaction comes from **2**: the e′-like MOs remain near-degenerate even when one is occupied in the "excited" state (0.053 eV gap between 1a″ and 1a′, Fig. 5). Furthermore, in the "ground" state, occupation of three-centre Ce–Ce σ-bonding MOs is not favoured: we found it impossible to converge UKS calculations by occupying the otherwise-empty LUMOs (Fig. 4, 5). We conclude that f–f interaction is insignificant in **2**. For the f-type orbitals of this cluster then, occupancy of MOs localised on the metal is preferred, rather than delocalised metal–metal bonding.

Conclusion

In conclusion, the formal oxidation state Ce(III)Ce(IV)Ce(IV) is assigned to **1** based on the finding that ionic interactions dictate the metal–ligand distances. Density functional calculations of the model trimer **2** yield a lowest-energy structure in excellent agreement with that from X-ray diffraction of **1**. The single unpaired electron is found to be localised on an orbital of f character on the NO_3-bearing Ce atom, confirming the Ce(III)-Ce(IV)Ce(IV) assignment.

Calculations also yield an alternative structure for **2**, just 18 kJ mol^{-1} higher in energy, where the f electron is shared between the pair of non-NO_3-bearing metal atoms. The associated change in the Ce_3 core geometry is very slight, but the metal-ligand distances are affected by the change in Ce oxidation state.

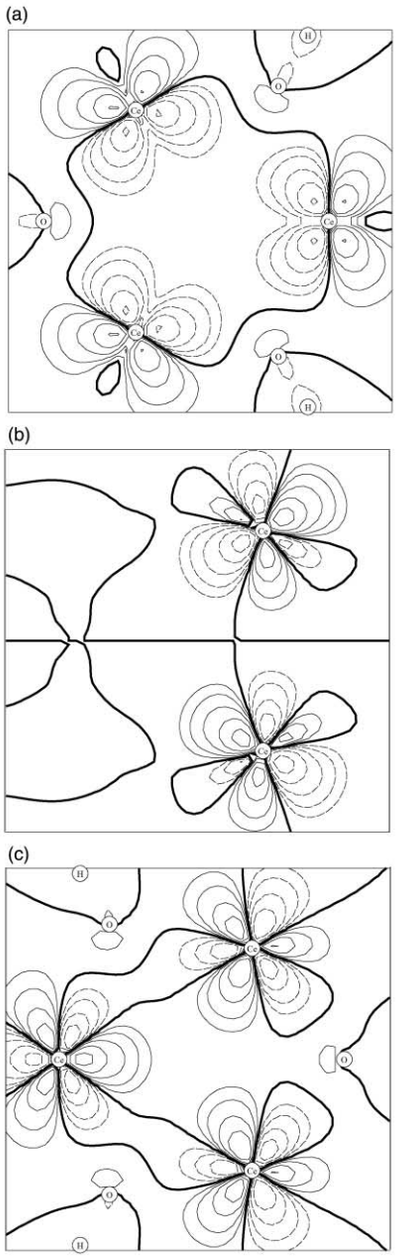

Fig. 3 MO contour plots through the Ce_3 plane of the lowest-lying UKS α MOs of Ce f character in the symmetrical D_{3h} compound **3**: (a) singly-occupied a'_1 HOMO and (b), (c) empty degenerate e′ LUMO (HOMO–LUMO gap of 15 kJ mol^{-1} = 0.16 eV). Thick lines are nodes, dashed and solid thin lines are contours of opposite parity.

Despite these changes in f occupancy, the Ce_3 core remains an almost equilateral triangle. We therefore conclude that the f-electron in **1** behaves as a spectator, barely affecting the core geometry and only influencing the ligands indirectly *via* ionic bonding. The excitation energy required to switch the f electron between metal centres is therefore low and **1** may be a useful component in molecular-scale electronic switching.

Experimental and computational

General procedures

All manipulations were carried out under vacuum or argon by Schlenk techniques. Solvents were dried and distilled over sodium-potassium alloy under argon prior to use and then condensed into a reaction flask under vacuum shortly before use. The ^{1}H NMR spectra were recorded using a Varian–400 (^{1}H, 400 MHz) instrument. Deuteriated benzene was dried over a K metal mirror and distilled prior to use. IR spectra

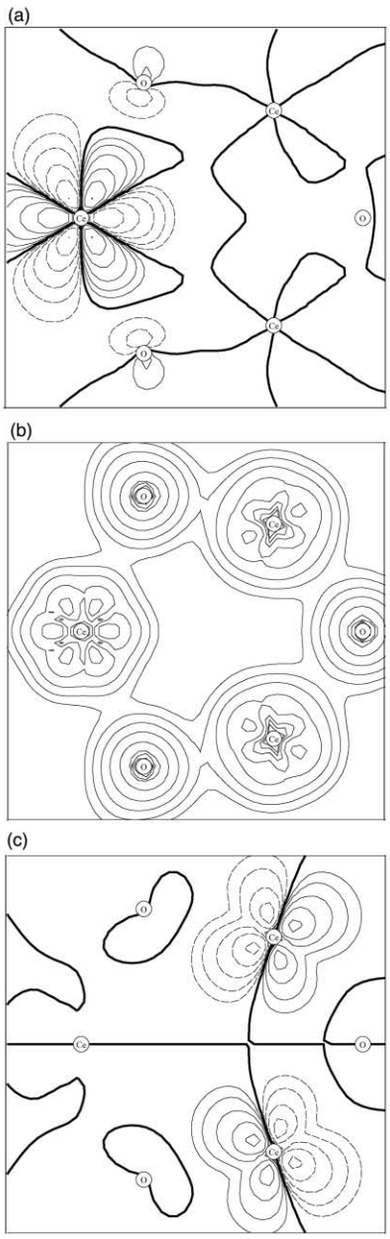

Fig. 4 MO contour plots through the Ce_3 plane of the lowest-lying UKS α MOs of Ce f character in the "ground" $^2A'$ state of the C_s model compound **2**: (a) singly-occupied 1a′ HOMO and (b) empty 2a′ LUMO (HOMO–LUMO gap of 87 kJ mol^{-1} = 0.90 eV). Also shown is (c) the empty 1a″ MO, which when filled gives the "excited" state of **2** (Fig. 5).

(500–4000 cm^{-1}) were recorded in 'Nujol', using KBr discs and a Perkin Elmer instrument. The compond $Sn(C_5H_3Bu^t_2\text{-}1,3)Me_3$ was prepared according to a literature method.[8]

Preparation and characterisation of 1

A solution of $[Ce(OBu^t)_4(THF)_2]$ (0.74 g, 1.28 mmol), $Ce(OBu^t)_3(NO_3)$ (0.27 g, 0.64 mmol) and $Sn(C_5H_3Bu^t_2\text{-}1,3)Me_3$ (0.65 g, 1.92 mmol) in hexane (100 cm^3) was heated under reflux for 24 h. The dark brown solution was then concentrated *in vacuo*. The green–brown crystals of **1** (0.57 g, 69%) crystallised from the solution at the ambient temperature. Anal. Calc. for $C_{46}H_{104}Ce_3NO_{13}$: C, 42.47; H, 8.00; N, 1.08. Found: C, 43.02; H, 8.16; N, 1.14%. NMR: ^1H (C_6D_6, 298 K): δ 17.34 (br s, 9H, μ_3-OBu^t), 8.55 (s, 9H, μ_3-OBu^t), 3.15 (s, 18H, OBu^t), 1.44 (s, 18H, OBu^t), 1.24 (s, 9H, μ-OBu^t), −4.68 (br s, 9H, OBu^t), −7.40 (br s, 18H, μ-OBu^t); IR ν_{max}/cm^{-1}: 1513 (s), 1273 (m), 1240 (m), 1028 (m), 978(s), 946 (m), 916 (s), 901 (s), 873 (s), 815 (s), 838 (m), 771 (m), 744 (s), 723 (m), 532(m), 503(m), 476(m); EI-MS: *m*/*z* 1093 ($[Ce(OBu^t)_3]_3O]^+$, 70%), 1020 ($[Ce(OBu^t)_3]_3O - OBu^t]^+$, 20%), 661 ($[Ce(OBu^t)_3]_3O - Ce(OBu^t)_3]^+$, 35%), 359 ($[Ce(OBu^t)_3]^+$, 95%), 57 ($[Bu^t]^+$, 100%).

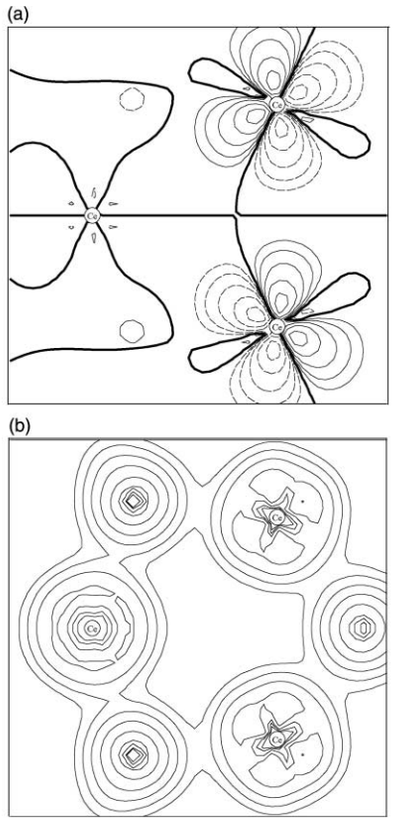

Fig. 5 MO contour plots through the Ce_3 plane of the lowest-lying UKS α MOs of Ce f character in the "excited" $^2A''$ state of the C_s model compound **2**: (a) singly-occupied 1a″ HOMO, (b) empty 1a′ LUMO (HOMO–LUMO gap of 5.3 kJ mol^{-1} = 0.055 eV).

Crystallography

Data set for **1** was measured on an Enraf-Nonius CAD4 at 173(2) K using monochromated Mo-Kα radiation. A single crystal of **1** *n*-hexane solvate, grown from hexane, was coated in oil and cooled. Corrections for absorption were made using ψ-scan measurements. Structure solution were made using SHELXS-86.[9] Refinement was based on F^2, with H atoms in riding mode, using SHELXL-93.[10] The C atoms of the *n*-hexane were only refined isotropically. No allowance was made for the H atoms of *n*-hexane.

Crystal data: $C_{40}H_{90}CeNO_{13}\cdot C_6H_{14}$, M = 1299.7, monoclinic, space group $P2_1/c$ (no.14), a = 18.266(2), b = 17.094(3), c = 19.994(4) Å, β = 105.34(1)°, U = 6021(2) $Å^3$, Z = 4, (Mo-Kα) = 2.28 mm^{-1}, D_c = 1.43 g cm^{-3}, T = 173 K. 10908 reflections measured, 10565 unique (R_{int} = 0.031). Refinement on all F^2. Final residuals wR_2 = 0.117 (all data), R_1 = 0.047 (for 7789 reflections with $[I > 2\sigma(I)]$).

CCDC reference number 174007.

See http://www.rsc.org/suppdata/dt/b1/b110247h/ for crystallographic data in CIF or other electronic format.

Computational details

Calculations were carried out using Unrestricted Kohn–Sham density functional theory (UKS) as implemented in the TURBOMOLE[11] program. The gradient-corrected BP86 functional[12] was employed, as it gives a reasonably reliable account of electron correlation in metal–ligand systems. A Split-Valence basis with one polarisation function (SVP) was used for H, O and F.[13] Ce was represented by 12 active electrons ($5s^25p^66s^24f^2$) around a 46-electron [Kr]$4d^{10}$ effective core potential. For the active electrons, a Split-Valence basis was

used with polarisation functions for the s, p and d but not f shells: (7s6p5d4f)/[5s4p3d2f].[13]

Geometries of the $^2A'$ and $^2A''$ states of **2** and the $^2A'_1$ state of **3** were optimised in UKS-BP86/SVP to a gradient norm of less than 10^{-3} E_h/Bohr (1 E_h (Hartree) = 2625.5 kJ mol^{-1}; 1 Bohr = 0.52918 Å); the energy convergence criteria for individual self-consistent steps was 10^{-6} E_h. Redundant internal coordinates were used for efficient optimisation.[14] No vertical energy differences were quoted: ΔE are 'adiabatic' in the sense that they are from optimised geometry to optimised geometry.

In unpublished preparatory work, we applied the same computational technique to small model dimers $[\{CeF_2(\mu\text{-}OH)\}_2]$ and $[\{Ce(C_5H_5)_2(\mu\text{-}OH)\}_2]$ and found excellent agreement with X-ray structures of $[\{Ce(\eta^5\text{-}C_5H_3Bu^t_2\text{-}1,3)_2(\mu\text{-}OMe)\}_2]$.[4] This indicates that alkoxy ligands are not significant for establishing the geometric and electronic structure of the metallic core and justifies our substitution of alkoxy with hydroxy ligands to give the model trimers **2** and **3**. With 425 and 385 Cartesian basis functions respectively, the model trimers still represented challenging calculations.

The lowest energy states calculated for **2** and **3** showed spin expectation values typical for a spin-pure UKS doublet ($\langle S^2 \rangle$ = 0.75). The "excited" $^2A''$ state of **2** was calculated to be spin-contaminated ($\langle S^2 \rangle$ = 0.87), which is not unusual for a partially occupied manifold of metallic orbitals, as here.

Acknowledgements

We thank Trinity College Dublin, Enterprise Ireland and EPSRC for support.

References

1 (*a*) F. L. Carter, R. E. Siakowski H. Wohltjen, *Molecular Electronic Devices*, North-Holland, Amsterdam, 1988; (*b*) C. W. Spangler and K. O. Havelka, *New J. Chem.*, 1991, **15**, 125; (*c*) J. S. Lindsey, *New J. Chem.*, 1991, **15**, 153; (*d*) R. M. Metzger and C. A. Panetta, *New J. Chem.*, 1991, **15**, 209; (*e*) M. A. Reed, *Proc. IEEE*, 1999, **87**, 652.
2 (*a*) D. Gatteschi, L. Pardi, A. L. Barra, A. Muller and J. Doring, *Nature*, 1991, **354**, 463; (*b*) S. Dibella, I. L. Fragalà, M. A. Ratner and T. J. Marks, *Mol. Biomol. Electron.*, 1994, **240**, 223.
3 W. J. Evans, T. J. Deming, J. M. Olofson and J. W. Ziller, *Inorg. Chem.*, 1989, **28**, 4027.
4 Y. K. Gun'ko, P. B. Hitchcock and M. F. Lappert, *J. Organomet. Chem.*, 1995, **499**, 213.
5 K. Yunlu, P. S. Gradeff, N. Edelstein, W. Kot, G. Shalimoff, W. E. Streib, B. A. Vaartstra and K. G. Caulton, *Inorg. Chem.*, 1991, **30**, 2317.
6 T. A. Beineke and J. Delgaudio, *Inorg. Chem.*, 1968, **7**, 715.
7 M. Ul-Haque, C. N. Caughlan, F. A. Hart and R. VanNice, *Inorg. Chem.*, 1971, **10**, 115.
8 M. A. Lyle and S. R. Stobart, *Inorg. Synth.*, 1977, **17**, 178.
9 G. M. Sheldrick, SHELXS 86, Program for the Solution of Crystal Structures, University of Göttingen, 1993.
10 G. M. Sheldrick, SHELXL 93, Program for Crystal Structures Refinement, University of Göttingen, 1993.
11 (*a*) O. Treutler and R. Ahlrichs, *J. Chem. Phys.*, 1995, **102**, 346; (*b*) R. Ahlrichs, M. Bär, M. Häser, H. Horn and C. Kölmel, *Chem. Phys. Lett.*, 1989, **162**, 165.
12 A. D. Becke, *Phys. Rev. A*, 1988, **38**, 3098; J. P. Perdew, *Phys. Rev. B*, 1986, **33**, 8822; J. P. Perdew, *Phys. Rev. B*, 1986, **34**, 7406(E).
13 A. Schäfer, H. Horn and R. Ahlrichs, *J. Chem. Phys.*, 1992, **97**, 2571; ftp://ftp.chemie.uni-karlsruhe.de/pub/basen.
14 M. v. Arnim and R. Ahlrichs, *J. Chem. Phys.*, 1999, **111**, 9183.